



0020-7683(94)E0011-J

INTERACTION BETWEEN A MAIN-CRACK AND A PARALLEL MICRO-CRACK IN AN ORTHOTROPIC PLANE ELASTIC SOLID

YI-HENG CHEN

Institute of Engineering Mechanics, Xi'an Jiao-tong University, Xi'an, 710049, P.R. China

and

NORIO HASEBE

Department of Civil Engineering, Nagoya Institute of Technology, Gokiso-cho,
Showa-ku, Nagoya 466, Japan

(Received 15 May 1993; in revised form 10 January 1994)

Abstract—This paper deals with the elastic interaction between a main-crack and a parallel micro-crack in an orthotropic plane elastic solid. The pseudo-traction method proposed by Chen [*Engng Fract. Mech.* **20**, 591–597 and 767–776 (1984a, b)], and Horii and Nemat-Nasser [*Int. J. Solids Structures* **21**, 731–745 (1985)] in isotropic cases is extended into orthotropic cases. After introducing two kinds of fundamental solutions, a system of Fredholm integral equations is derived from which the interaction effect of the release of residual stresses due to near-tip micro-cracking is evaluated. Numerical results are shown in figures and tables. Some useful conclusions are discussed.

1. INTRODUCTION

The mechanism of fracture of a material in the microscale is always concerned with micro defects such as cracks, voids and inclusions among which micro-cracking has received considerable attention in recent years. Elastic interaction effect between a main-crack and micro-cracks in isotropic materials was well studied and a number of analytical solutions were reported in the literature [see e.g. Hoagland and Embury (1980); Gross (1982); Chudnovsky and Kachanov (1983); Chudnovsky *et al.* (1987); Rose (1986); Horii and Nemat-Nasser (1985, 1987); Gong and Horii (1989); Gong and Meguid (1991); Ukadgaonker and Naik (1991a,b); Chudnovsky and Wu (1991)]. A history review was performed by Kachanov (1993). However, the same problems in anisotropic cases have just brought a renewed interest [see e.g. Binienda *et al.* (1991); Hwu (1991)].

A method called the “pseudo-traction” method was proposed by Horii and Nemat-Nasser (1985). In fact, almost the same method was proposed a little earlier by Chen (1984a,b). The method was modified by Horii and Nemat-Nasser (1987) for the case when micro-cracks are situated very close to the main-crack tip.

The aim of the present work is to extend the method into anisotropic cases with a micro-crack parallel to a main-crack. After introducing two kinds of fundamental solutions, a system of Fredholm integral equations is derived. The residual stresses at the location of the near-tip micro-cracking presented by Sih and Chen (1981) are released and the interaction effect of the release is then evaluated.

A particular kind of material is considered in detail which is concerned with the orthotropic material used by Bowie and Freese (1972). The effect of material and geometrical parameters upon the change in the stress intensity factors is discussed. Numerical results are shown in figures and tables. A comparison with those reported in the literature is performed for giving the verification.

It is found that the parameters of orthotropic materials have no influence on the interaction effect under purely Mode I loading conditions when the main-crack and the micro-crack are collinear along the axis of material symmetry. However, the parameters significantly influence the interaction effect when a non-collinear micro-crack is created

very close to the tip of the main-crack. The dependence of the effect on the orthotropic parameters is studied in detail which is found to be very sensitive in some ranges of the parameters.

It is also found that the interaction effect may be either amplification or shielding as in isotropic cases (Rose, 1986; Gong and Horii, 1989). However, the transition from an amplification effect to a shielding effect is significantly influenced by the parameters of orthotropic materials.

2. FUNDAMENTAL SOLUTIONS

The investigation performed in the present paper starts from the following fundamental solutions (see Fig. 1(a,b)) in which a crack of length $2a$ in an anisotropic plane elastic solid is considered.

From the well-known Lekhnitskii theorem (1963), the stress representations in an anisotropic plane elastic solid can be put in the following form :

$$\sigma_x = 2\text{Re} (S_1^2\phi'(Z_1) + S_2^2\psi'(Z_2)) \tag{1a}$$

$$\sigma_y = 2\text{Re} (\phi'(Z_1) + \psi'(Z_2)) \tag{1b}$$

$$\sigma_{xy} = -2\text{Re} (S_1\phi'(Z_1) + S_2\psi'(Z_2)) \tag{1c}$$

where $\phi(Z_1)$ and $\psi(Z_2)$ are complex potentials with respect to the complex arguments Z_1 and Z_2 , respectively; the prime denotes differentiation with the respective complex arguments Z_1 or Z_2 ; $Z_1 = x + S_1y$ and $Z_2 = x + S_2y$. S_1, S_2 and their conjugates are roots of the characteristic equation which are either complex or purely imaginary and cannot be real (Lekhnitskii, 1963) :

$$b_{11}S^4 - 2b_{16}S^3 + (2b_{12} + b_{66})S^2 - 2b_{26}S + b_{22} = 0 \tag{2}$$

where $b_{11}, b_{16}, b_{12}, b_{26}, b_{66}$, and b_{22} are real constants of the anisotropic material.

(A). The first kind of fundamental solution is considered in Fig. 1(a) in which the loading involves only normal concentrated traction applied on both the crack surfaces in the y -direction. Hence, the shear stress σ_{xy} vanishes everywhere along the line of loading symmetry $y = 0$, which is not necessarily the axis of material symmetry unless orthotropic is invoked (Sih and Chen, 1981).

Using eqn (1c), the condition $\sigma_{xy} = 0$ for $Z_1 = Z_2 = t$ on the real axis gives

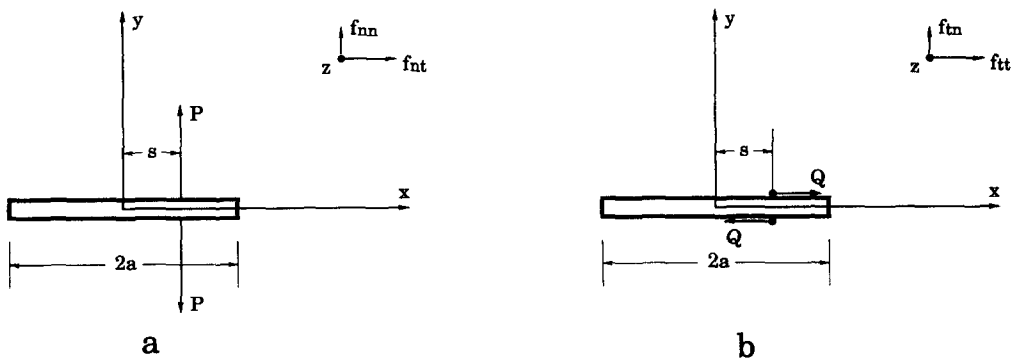


Fig. 1. Normal concentrated tractions or shear concentrated tractions acting on both faces of a typical crack.

$$S_1\Phi_1(t) + S_2\Psi_1(t) = 0 \quad \text{for all } t \tag{3a}$$

or

$$\Psi_1(t) = -\frac{S_1}{S_2}\Phi_1(t) \quad \text{for all } t \tag{3b}$$

where

$$\Phi_1(Z_1) = \phi'(Z_1) \tag{4a}$$

$$\Psi_1(Z_2) = \psi'(Z_2). \tag{4b}$$

Letting Z_1 and Z_2 approach the upper ($y > 0$) and lower ($y < 0$) side of the crack, eqn (1b) yields the following relations for $|t| < a$:

$$\sigma_y^+ = \left(\frac{S_2 - S_1}{S_2}\right)\Phi_1^+(t) + \left(\frac{\overline{S_2 - S_1}}{S_2}\right)\overline{\Phi_1^-}(t) \tag{5a}$$

$$\sigma_y^- = \left(\frac{S_2 - S_1}{S_2}\right)\Phi_1^-(t) + \left(\frac{\overline{S_2 - S_1}}{S_2}\right)\overline{\Phi_1^+}(t) \tag{5b}$$

where the superscripts + and - denote the boundary values of those quantities on the upper and lower side of the crack, respectively.

Following the work performed by Sih and Chen (1981), the problem stated in Fig. 1(a) can be reduced to the following Riemann-Hilbert problem:

$$\left\{ \left(\frac{S_2 - S_1}{S_2}\right)\Phi_1(t) + \left(\frac{\overline{S_2 - S_1}}{S_2}\right)\overline{\Phi_1(t)} \right\}^+ + \left\{ \left(\frac{S_2 - S_1}{S_2}\right)\Phi_1(t) + \left(\frac{\overline{S_2 - S_1}}{S_2}\right)\overline{\Phi_1(t)} \right\}^- = -2P\delta(t-s) \quad \text{for } |t| < a \tag{6a}$$

$$\left\{ \left(\frac{S_2 - S_1}{S_2}\right)\Phi_1(t) - \left(\frac{\overline{S_2 - S_1}}{S_2}\right)\overline{\Phi_1(t)} \right\}^+ - \left\{ \left(\frac{S_2 - S_1}{S_2}\right)\Phi_1(t) - \left(\frac{\overline{S_2 - S_1}}{S_2}\right)\overline{\Phi_1(t)} \right\}^- = 0 \quad \text{for } |t| < a \tag{6b}$$

where δ denotes the Dirac function.

Assuming the stress at infinity to vanish, then $\Phi_1(Z_1) \rightarrow o(1/Z_1)$ for large values of Z_1 , and the solutions to eqns (6a, b) are:

$$\left(\frac{S_2 - S_1}{S_2}\right)\Phi_1(Z_1) + \left(\frac{\overline{S_2 - S_1}}{S_2}\right)\overline{\Phi_1(Z_1)} = -\frac{P}{i\pi(s - Z_1)} \sqrt{\frac{s^2 - a^2}{Z_1^2 - a^2}} \tag{7a}$$

$$\left(\frac{S_2 - S_1}{S_2}\right)\Phi_1(Z_1) - \left(\frac{\overline{S_2 - S_1}}{S_2}\right)\overline{\Phi_1(Z_1)} = 0. \tag{7b}$$

Once $\overline{\Phi_1(Z_1)}$ is eliminated from eqns (7a, b), the following result is given:

$$\Phi_1(Z_1) = -\frac{PS_2}{2\pi(s - Z_1)(S_2 - S_1)} \sqrt{\frac{a^2 - s^2}{Z_1^2 - a^2}}. \tag{8a}$$

The similar procedure can be performed for $\Psi_1(Z_2)$, without going into details, it follows that

$$\Psi_1(Z_2) = -\frac{PS_1}{2\pi(s-Z_2)(S_1-S_2)} \sqrt{\frac{a^2-s^2}{Z_2^2-a^2}} \tag{8b}$$

Consequently, the stresses at any point in the xy -plane can be given as follows (Bowie and Freese, 1972):

$$f_{m} - if_{nt} = \sigma_y - i\sigma_{xy} = (1+iS_1)\Phi_1(Z_1) + (1+iS_2)\Psi_1(Z_2) + (1+i\bar{S}_1)\overline{\Phi_1(Z_1)} + (1+i\bar{S}_2)\overline{\Psi_1(Z_2)}. \tag{9}$$

From eqn (8a) the stress intensity factors at both tips are given (Sih and Liebowitz, 1968):

$$K_1(\text{Right}) = 2\sqrt{2} \left(\frac{S_2-S_1}{S_2} \right) \lim_{Z_1 \rightarrow a} \sqrt{Z_1-a} \Phi_1(Z_1) \tag{10a}$$

$$K_1(\text{Left}) = 2\sqrt{2} \left(\frac{S_2-S_1}{S_2} \right) \lim_{Z_1 \rightarrow -a} i \sqrt{Z_1+a} \Phi_1(Z_1). \tag{10b}$$

(B). The second kind of fundamental solution is considered in Fig. 1(b) in which the skew-symmetric loading involves only shear concentrated traction applied on both crack surfaces in the x -direction.

Using eqn (1b), the condition $\sigma_y = 0$ for $Z_1 = Z_2 = t$ on the real axis gives

$$\Phi_2(t) + \Psi_2(t) = 0 \quad \text{for all } t. \tag{11a}$$

or

$$\Psi_2(t) = -\Phi_2(t) \quad \text{for all } t. \tag{11b}$$

Hence,

$$\sigma_{xy}^+ = (S_2-S_1)\Phi_2^+(t) + (\bar{S}_2-\bar{S}_1)\overline{\Phi_2^-(t)} \quad \text{for } |t| < a \tag{12a}$$

$$\sigma_{xy}^- = (S_2-S_1)\Phi_2^-(t) + (\bar{S}_2-\bar{S}_1)\overline{\Phi_2^+(t)} \quad \text{for } |t| < a \tag{12b}$$

and the following Riemann–Hilbert problem is reduced:

$$\{(S_2-S_1)\Phi_2(t) + (\bar{S}_2-\bar{S}_1)\overline{\Phi_2(t)}\}^+ + \{(S_2-S_1)\Phi_2(t) + (\bar{S}_2-\bar{S}_1)\overline{\Phi_2(t)}\}^- = -2Q\delta(t-s) \quad \text{for } |t| < a \tag{13a}$$

$$\{(S_2-S_1)\Phi_2(t) - (\bar{S}_2-\bar{S}_1)\overline{\Phi_2(t)}\}^+ - \{(S_2-S_1)\Phi_2(t) - (\bar{S}_2-\bar{S}_1)\overline{\Phi_2(t)}\}^- = 0 \quad \text{for } |t| < a. \tag{13b}$$

The solution of eqns (13a) and (13b) is:

$$\Phi_2(Z_1) = -\frac{Q}{2\pi(s-Z_1)(S_2-S_1)} \sqrt{\frac{a^2-s^2}{Z_1^2-a^2}} \tag{14a}$$

Repeating the above procedure for $\Psi_2(Z_2)$, it follows that

$$\Psi_2(Z_2) = -\frac{Q}{2\pi(s-Z_2)(S_1-S_2)} \sqrt{\frac{a^2-s^2}{Z_2^2-a^2}} \tag{14b}$$

The stress intensity factors at both tips can then be evaluated (Sih and Liebowitz, 1968):

$$K_2(\text{Right}) = 2\sqrt{2}(S_2-S_1) \lim_{Z_1 \rightarrow a} \sqrt{Z_1-a} \Phi_2(Z_1) \tag{15a}$$

and

$$K_2(\text{Left}) = 2\sqrt{2}(S_2 - S_1) \lim_{Z_1 \rightarrow -a} i \sqrt{Z_1 + a} \Phi_2(Z_1). \tag{15b}$$

The stresses at any point in the xy -plane can be given as follows :

$$f_{in} - if_{it} = \sigma_y - i\sigma_{xy} = (1 + iS_1)\Phi_2(Z_1) + (1 + iS_2)\Psi_2(Z_2) + (1 + i\overline{S_1})\overline{\Phi_2(Z_1)} + (1 + i\overline{S_2})\overline{\Psi_2(Z_2)}. \tag{16}$$

3. FREDHOLM INTEGRAL EQUATIONS FOR SOLVING THE INTERACTION PROBLEM BETWEEN A MAIN-CRACK AND A MICRO-CRACK

Considering an arbitrarily located micro-crack of length $2a_1$ (Fig. 2) which is near the right tip of the main-crack and also parallel to the main-crack. The main-crack is assumed much larger than the length of the micro-crack and the distance between the right tip of the main-crack and the center of the micro-crack (the so-called small-scale approach) :

$$a \gg a_1, \quad a \gg d. \tag{17}$$

Using the ‘‘pseudo-traction’’ methods proposed by Chen (1984a,b) and Horii and Nemat-Nasser (1985) in isotropic cases, the present problem shown in Fig. 2 is decomposed into two subproblems, each of which contains one single crack. It is assumed that $p(t)$ and $q(t)$ indicate the really residual stresses to be released on the location of the micro-crack which are known functions and that $P_0(x)$, $Q_0(x)$, $P_1(t)$ and $Q_1(t)$ are so-called pseudo-tractions (Horii and Nemat-Nasser, 1985; Gong and Horii, 1989) to be determined.

Using the fundamental solutions mentioned in the above section and the superimposing technique, the above problem can be reduced to the following Fredholm integral equations as Chen (1984a,b) did in isotropic cases :

$$P_0(s) + \int_{-a_1}^{+a_1} P_1(t) f_{nn,10}(t, s) dt + \int_{-a_1}^{+a_1} Q_1(t) f_{in,10}(t, s) dt = 0 \quad (-a < s < a) \tag{18a}$$

$$Q_0(s) + \int_{-a_1}^{+a_1} P_1(t) f_{nt,10}(t, s) dt + \int_{-a_1}^{+a_1} Q_1(t) f_{it,10}(t, s) dt = 0 \quad (-a < s < a) \tag{18b}$$

$$P_1(t) + \int_{-a}^{+a} P_0(s) f_{nn,01}(s, t) ds + \int_{-a}^{+a} Q_0(s) f_{in,01}(s, t) ds = p(t) \quad (-a_1 < t < a_1) \tag{18c}$$

$$Q_1(t) + \int_{-a}^{+a} P_0(s) f_{nt,01}(s, t) ds + \int_{-a}^{+a} Q_0(s) f_{it,01}(s, t) ds = q(t) \quad (-a_1 < t < a_1) \tag{18d}$$

where the eight kernel functions $(f_{nn,10})$, $(f_{in,10})$, $(f_{nt,10})$, $(f_{it,10})$, $(f_{nn,01})$, $(f_{in,01})$, $(f_{nt,01})$, and $(f_{it,01})$ have been given by eqns (9) and (16), respectively. The subscripts $n, t, 0, 1$ have definite meanings : n indicates the normal quantity ; t indicates the tangential quantity, 0

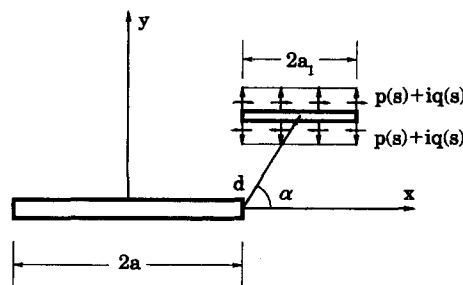


Fig. 2. A micro-crack parallel to a main-crack.

indicates the main-crack; 1 indicates the micro-crack. For example, $f_{n,10}(t, s)$ means the contribution of the unit normal concentrated traction acting on the micro-crack surfaces at the point t to the main-crack in the tangential direction at the point s (Chen, 1984a,b).

Using the Chebyshev numerical integration, the following linear system with $4M$ unknowns $P_0(s_i)$, $Q_0(s_i)$, $P_1(t_j)$ and $Q_1(t_j)$ ($i, j = 1, 2, \dots, M$) can be given

$$P_0(s_i) + \sum_{j=1}^M P_1(t_j) f_{n,10}(t_j, s_i) \delta_j + \sum_{j=1}^M Q_1(t_j) f_{t,10}(t_j, s_i) \delta_j = 0 \quad i = 1, 2, \dots, M \quad (19a)$$

$$Q_0(s_i) + \sum_{j=1}^M P_1(t_j) f_{n,10}(t_j, s_i) \delta_j + \sum_{j=1}^M Q_1(t_j) f_{t,10}(t_j, s_i) \delta_j = 0 \quad i = 1, 2, \dots, M \quad (19b)$$

$$P_1(t_j) + \sum_{i=1}^M P_0(s_i) f_{n,01}(s_i, t_j) \delta_i + \sum_{i=1}^M Q_0(s_i) f_{t,01}(s_i, t_j) \delta_i = p(t_j) \quad j = 1, 2, \dots, M \quad (19c)$$

$$Q_1(t_j) + \sum_{i=1}^M P_0(s_i) f_{n,01}(s_i, t_j) \delta_i + \sum_{i=1}^M Q_0(s_i) f_{t,01}(s_i, t_j) \delta_i = q(t_j) \quad j = 1, 2, \dots, M \quad (19d)$$

where

$$s_i = a \cdot \cos \frac{(2i-1)\pi}{2M} \quad (20a)$$

$$t_j = a_1 \cdot \cos \frac{(2j-1)\pi}{2M} \quad (20b)$$

$$\delta_i = \frac{a\pi}{M} \cdot \sin \frac{(2i-1)\pi}{2M} \quad (20c)$$

$$\delta_j = \frac{a_1\pi}{M} \cdot \sin \frac{(2j-1)\pi}{2M} \quad (20d)$$

and δ_i and δ_j are the array encountered in the Chebyshev integral rule.

Once the system is solved, the incremental values of stress intensity factors at both tips of the main-crack and the stress intensity factors at both tips of the micro-crack can be evaluated by using the following quadrature rule (Erdogan, 1978):

$$\int_{-a}^{+a} \frac{f(x) dx}{\sqrt{a^2-x^2}} \approx \frac{\pi}{M} \sum_{m=1}^M f \left\{ a \cdot \cos \frac{(2m-1)\pi}{2M} \right\} \quad (21a)$$

and

$$\int_{-a_1}^{+a_1} \frac{g(t) dt}{\sqrt{a_1^2-t^2}} \approx \frac{\pi}{M} \sum_{m=1}^M g \left\{ a_1 \cdot \cos \frac{(2m-1)\pi}{2M} \right\}. \quad (21b)$$

Finally, it follows that: for the main-crack

$$\Delta K_1^{\text{Right}} = \frac{\sqrt{a}}{M} \sum_{m=1}^M P_0 \left\{ a \cdot \cos \frac{(2m-1)\pi}{2M} \right\} \cdot \left\{ 1 + \cos \frac{(2m-1)\pi}{2M} \right\} \quad (22a)$$

$$\Delta K_1^{\text{Left}} = \frac{\sqrt{a}}{M} \sum_{m=1}^M P_0 \left\{ a \cdot \cos \frac{(2m-1)\pi}{2M} \right\} \cdot \left\{ 1 - \cos \frac{(2m-1)\pi}{2M} \right\} \quad (22b)$$

$$\Delta K_2^{\text{Right}} = \frac{\sqrt{a}}{M} \sum_{m=1}^M Q_0 \left\{ a \cdot \cos \frac{(2m-1)\pi}{2M} \right\} \cdot \left\{ 1 + \cos \frac{(2m-1)\pi}{2M} \right\} \quad (22c)$$

$$\Delta K_2^{\text{Left}} = \frac{\sqrt{a}}{M} \sum_{m=1}^M Q_0 \left\{ a \cdot \cos \frac{(2m-1)\pi}{2M} \right\} \cdot \left\{ 1 - \cos \frac{(2m-1)\pi}{2M} \right\} \quad (22d)$$

and for the micro-crack

$$K_1^{\text{Right}} = \frac{\sqrt{a_1}}{M} \sum_{m=1}^M P_1 \left\{ a_1 \cdot \cos \frac{(2m-1)\pi}{2M} \right\} \cdot \left\{ 1 + \cos \frac{(2m-1)\pi}{2M} \right\} \tag{23a}$$

$$K_1^{\text{Left}} = \frac{\sqrt{a_1}}{M} \sum_{m=1}^M P_1 \left\{ a_1 \cdot \cos \frac{(2m-1)\pi}{2M} \right\} \cdot \left\{ 1 - \cos \frac{(2m-1)\pi}{2M} \right\} \tag{23b}$$

$$K_2^{\text{Right}} = \frac{\sqrt{a_1}}{M} \sum_{m=1}^M Q_1 \left\{ a_1 \cdot \cos \frac{(2m-1)\pi}{2M} \right\} \cdot \left\{ 1 + \cos \frac{(2m-1)\pi}{2M} \right\} \tag{23c}$$

$$K_2^{\text{Left}} = \frac{\sqrt{a_1}}{M} \sum_{m=1}^M Q_1 \left\{ a_1 \cdot \cos \frac{(2m-1)\pi}{2M} \right\} \cdot \left\{ 1 - \cos \frac{(2m-1)\pi}{2M} \right\}. \tag{23d}$$

4. THE RELEASE OF RESIDUAL STRESSES DUE TO THE NEAR-TIP MICRO-CRACKING

Assuming the specified self-balancing normal traction σ_0 on the main-crack surfaces, the stress intensity factors at both tips and the near-tip stress fields are given by Sih and Chen (1981):

$$K_1^0(\text{Right and Left}) = \sigma_0 \sqrt{a} \tag{24}$$

$$\sigma_x = \frac{K_1^0}{\sqrt{2r}} \operatorname{Re} \left\{ \frac{S_1 S_2}{S_1 - S_2} \left(\frac{S_2}{\sqrt{\cos \theta + S_2 \cdot \sin \theta}} - \frac{S_1}{\sqrt{\cos \theta + S_1 \cdot \sin \theta}} \right) \right\} + O(r^0) \tag{25a}$$

$$\sigma_y = \frac{K_1^0}{\sqrt{2r}} \operatorname{Re} \left\{ \frac{1}{S_1 - S_2} \left(\frac{S_1}{\sqrt{\cos \theta + S_2 \cdot \sin \theta}} - \frac{S_2}{\sqrt{\cos \theta + S_1 \cdot \sin \theta}} \right) \right\} + O(r^0) \tag{25b}$$

$$\sigma_{xy} = \frac{K_1^0}{\sqrt{2r}} \operatorname{Re} \left\{ \frac{S_1 S_2}{S_1 - S_2} \left(\frac{1}{\sqrt{\cos \theta + S_1 \cdot \sin \theta}} - \frac{1}{\sqrt{\cos \theta + S_2 \cdot \sin \theta}} \right) \right\} + O(r^0) \tag{25c}$$

where

$$r = \sqrt{(x-a)^2 + y^2} \tag{26a}$$

$$\theta = \tan^{-1} \left(\frac{y}{x-a} \right) \quad \text{for } x > a \tag{26b}$$

$$\theta = \pi + \tan^{-1} \left(\frac{y}{x-a} \right) \quad \text{for } x < a, y > a \tag{26c}$$

$$\theta = -\pi + \tan^{-1} \left(\frac{y}{x-a} \right) \quad \text{for } x < a \text{ and } y < a. \tag{26d}$$

The residual stresses on the micro-crack location to be released can be expanded into the Taylor series form as treated by Gong and Horii (1989) from which the right sides of eqns (19c, d), i.e. $p(t_j)$ and $q(t_j)$, are evaluated by taking the dominant terms in the series and then the so-called 0th order solution and the first order solution are given. However, this treatment may introduce some unexpected errors when the micro-crack is situated very close to the main-crack tip [see e.g. Table 1 in Gong and Horii (1989)]. In the present investigation, the residual stresses to be released are evaluated directly from eqns (25b, c) which can give any desirable accuracy.

Table 1. The normalized stress intensity factor K_1^{MA}/K_1^0 at the right tip of the main-crack influenced by a collinear micro-crack when setting $\beta_1\beta_2 = 1.00001$ in eqn (29a) and $\beta_1 \approx \beta_2$ in eqn (29b)

d/a_1	Exact	Approximate (first order) (Gong and Horii, 1989)	Present solutions
1.1	1.652	1.329	1.651
1.2	1.387	1.260	1.386
1.3	1.274	1.211	1.273
1.4	1.209	1.174	1.209
1.5	1.167	1.147	1.167
2.0	1.076	1.074	1.076

5. NUMERICAL RESULTS AND DISCUSSION

The analysis method presented in the above sections is programmed and a particular kind of anisotropic material, i.e. an orthotropic material with purely imaginary characteristic roots, is considered in detail for obtaining the major features of the interaction problem. This kind of material was used numerically by Bowie and Freese (1972) and Chen and Hahn (1989) for unidirectional fibre reinforced composites and the characteristic equation (2) is simplified to the following form :

$$b_{11}S^4 + (2b_{12} + b_{66})S^2 + b_{22} = 0. \tag{27}$$

Under some circumstances, the characteristic roots are purely imaginary :

$$S_1 = i\beta_1 \tag{28a}$$

$$S_2 = i\beta_2 \tag{28b}$$

where $\beta_1 > 0$ and $\beta_2 > 0$, and

$$\beta_1\beta_2 = \sqrt{\frac{E_{11}}{E_{22}}} \tag{29a}$$

$$\beta_1 + \beta_2 = \sqrt{2} \left\{ \sqrt{\frac{E_{11}}{E_{22}}} + \frac{E_{11}}{2\mu_{12}} - \nu_{12} \right\}^{1/2} \tag{29b}$$

in which E_{11} and E_{22} are the moduli of elasticity in the material principle directions, i.e x and y axes, respectively ; ν_{12} is the Poisson's ratio ; μ_{12} is the shear modulus in the xy -plane.

It should be mentioned that another kind of characteristic root could be found from eqn (27) as treated by Sih and Chen (1981). However, in this paper only the purely imaginary roots (28a, b) are considered.

Assuming that a main-crack in the orthotropic material is under purely Mode I loading conditions and that the residual stresses due to a parallel near-tip micro-cracking are released, the interaction effect can then be represented by the normalized stress intensity factors at the right tip of the main-crack :

$$K_1^{MA}/K_1^0 = 1 + \Delta K_1^{Right}/K_1^0 \tag{30a}$$

$$K_2^{MA}/K_1^0 = \Delta K_2^{Right}/K_1^0. \tag{30b}$$

It is seen from Tables 1 and 2 that the numerical results from the present investigation coincide well with those in isotropic cases (Gong and Horii, 1989) when setting β_1 and β_2 or $\sqrt{E_{11}/E_{22}}$ to be the limit values, i.e. $\beta_1 = 1$ and $\beta_2 \rightarrow 1$ or $\sqrt{E_{11}/E_{22}} \approx 1$. Consequently, the analysis method proposed in the present investigation is verified which provides a

Table 2. The normalized stress intensity factors K_1^{MA}/K_1^0 at the tips of a collinear micro-crack when setting $\beta_1 = 1$ and $\beta_2 \approx 1$ in eqns (29a, b)

d/a_1	Exact		Approximate (first order) (Gong and Horii, 1989)		Present solution	
	Right tip	Left tip	Right tip	Left tip	Right tip	Left tip
1.1	0.655	1.469	0.660	0.967	0.655	1.474
1.2	0.610	1.138	0.623	0.892	0.610	1.138
1.3	0.579	0.979	0.593	0.831	0.579	0.978
1.4	0.555	0.877	0.567	0.781	0.554	0.877
1.5	0.534	0.805	0.545	0.738	0.534	0.805
2.0	0.464	0.611	0.469	0.594	0.463	0.611

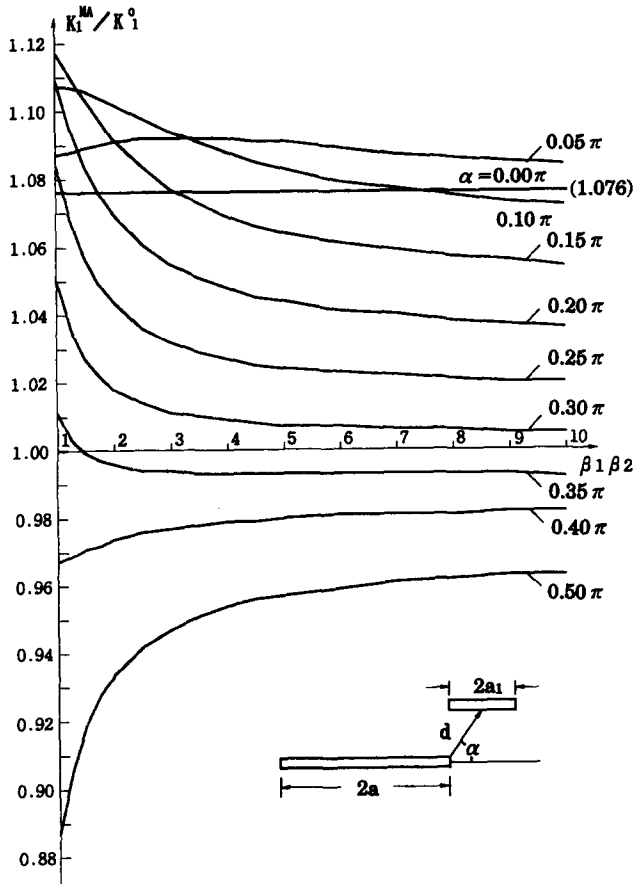


Fig. 3. The interaction effect K_1^{MA}/K_1^0 due to the parallel near-tip micro-cracking in an orthotropic elastic solid with $S_1 = i\beta_1$, $S_2 = i\beta_2$ assuming $a/a_1 = 100$, $d/a_1 = 2$, $\beta_1 = 1$, and $\beta_2 > 1$.

reasonable accuracy when the micro-crack is situated very close to the right tip of the main-crack.

Of the most interest is K_1^{MA}/K_1^0 against the angle α (see Fig. 2) and the parameter $\beta_1\beta_2(\sqrt{E_{11}/E_{22}})$ which is plotted in Fig. 3 for $\beta_1\beta_2 > 1$ and in Fig. 4 for $\beta_1\beta_2 < 1$, respectively, assuming $\beta_1 = 1$.

It is found from Figs 3 and 4 that there is no influence of the orthotropic parameter on the interaction effect K_1^{MA}/K_1^0 when the main-crack and micro-crack are collinear along the axis of material symmetry corresponding to $\alpha = 0$ and the results are just the same as those in isotropic cases. This phenomenon can be explained by considering the near-tip stress field (25b, c) as well as the complex potentials (8a, b) and (14a, b) in the limit cases of $\theta = 0$. It is seen that the residual stresses to be released for a collinear micro-crack become

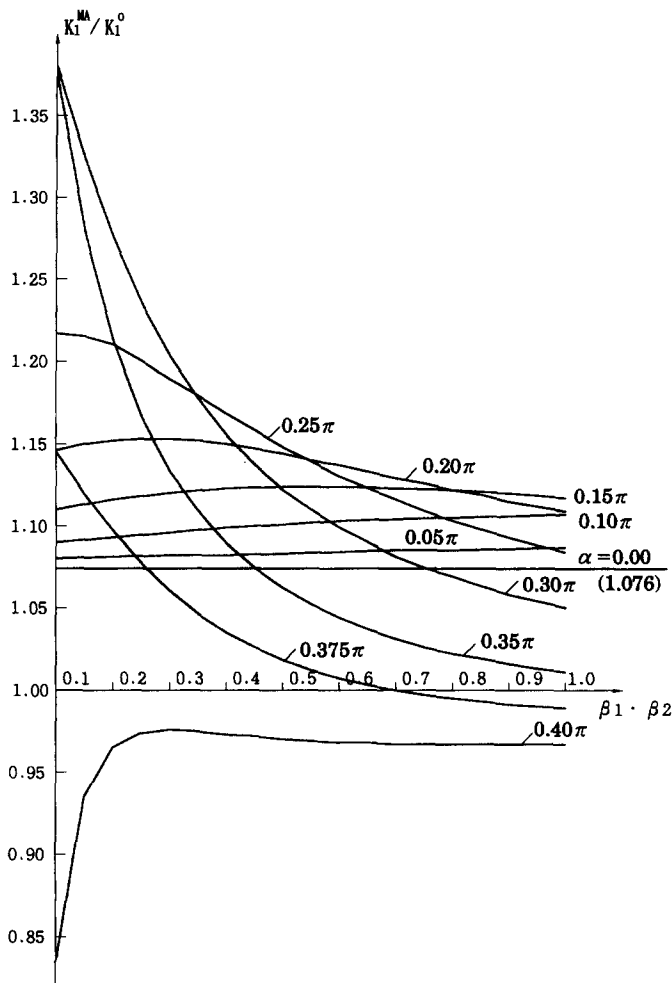


Fig. 4. The interaction effect K_I^{MA}/K_I^0 due to the parallel near-tip micro-cracking in an orthotropic elastic solid with $S_1 = i\beta_1$ and $S_2 = i\beta_2$ assuming $a/a_1 = 100$, $d/a_1 = 2$, $\beta_1 = 1$, and $\beta_2 < 1$.

$$\sigma_y(\theta = 0) = \frac{K_I^0}{\sqrt{2r}} \tag{31a}$$

$$\sigma_{xy}(\theta = 0) = 0 \tag{31b}$$

and the kernel functions in eqns (18a, b) become

$$f_{nn,01} = -\frac{1}{\pi(t-x)} \sqrt{\frac{a^2-t^2}{x^2-a^2}} \tag{32a}$$

$$f_{nn,10} = -\frac{1}{\pi(s-\bar{x})} \sqrt{\frac{a_1^2-s^2}{\bar{x}^2-a_1^2}} \tag{32b}$$

$$f_{ni,01} = f_{ni,10} = f_{n,01} = f_{n,10} = f_{u,01} = f_{u,10} = 0 \tag{32c}$$

where $\bar{x} = x - d - a$.

It is noted that all the terms of both sides of the Fredholm integral equations (18a-d) are independent of the parameters β_1 and β_2 . Therefore, the interaction effect of the release of the residual stresses (31a, b) due to the collinear near-tip micro-cracking will be independent of the parameters.

Table 3. The tendency of the normalized stress intensity factors K_1^{MA}/K_1^0 when setting $\beta_1 = 1$ and $\beta_2 \rightarrow \infty$ assuming $a/a_1 = 100$ and $d/a_1 = 2$

$\beta_1\beta_2$	10	25	64	100
α				
0.10 π	1.07171	1.06505	1.06233	1.06168
0.20 π	1.03638	1.03240	1.03076	1.03036
0.30 π	1.004973	1.003594	1.002978	1.002924
0.40 π	0.98184	0.98290	0.98326	0.98334
0.50 π	0.96345	0.96709	0.96846	0.96877

It is also found from Figs 3 and 4 that the influence of the parameter on the effect is not sensitive when the micro-crack is little diverged from the collinear situation, for example, $\alpha < 9^\circ$ (0.05π) in Fig. 3 and $\alpha < 18^\circ$ (0.10π) in Fig. 4. However, the influence increases very sharply as α increases since the angle distribution of the residual stresses to be released, i.e. eqns (25b, c), is seriously disturbed by the orthotropic parameters as α increases (Sih and Chen, 1981).

In Fig. 3 the sensitivity is found to be large in the range of $\beta_1\beta_2$ between 1 and 3 assuming $\beta_1 = 1$. However, the sensitivity becomes very small when $\beta_1\beta_2$ increases from 7. It seems that asymptotical values for the effect could be found when setting $\beta_2 \rightarrow \infty$.

Considering the complex potentials (8a, b) and (14a, b) and assuming $\beta_1 = 1$ and $\beta_2 \rightarrow \infty$, it follows that

$$\lim_{\beta_2 \rightarrow \infty} \Phi_1(z_1) = -\frac{P}{2\pi(s-z_1)} \sqrt{\frac{a^2-s^2}{z_1^2-a^2}} \tag{33a}$$

$$\lim_{\beta_2 \rightarrow \infty} \Psi_1(z_1) = 0 \quad \text{or} \quad 0(\beta_2^{-3}) \quad \text{for large } \beta_2 \tag{33b}$$

$$\lim_{\beta_2 \rightarrow \infty} \Phi_2(z_1) = 0 \quad \text{or} \quad 0(\beta_2^{-1}) \quad \text{for large } \beta_2 \tag{33c}$$

$$\lim_{\beta_2 \rightarrow \infty} \Psi_2(t_2) = 0 \quad \text{or} \quad 0(\beta_2^{-3}) \quad \text{for large } \beta_2 \tag{33d}$$

and

$$\lim_{\beta_2 \rightarrow \infty} \sigma_y = \frac{K_1^0}{\sqrt{2r}} \operatorname{Re} \left(\frac{1}{\sqrt{\cos \theta + s_1 \sin \theta}} \right) \tag{34a}$$

$$\lim_{\beta_2 \rightarrow \infty} \sigma_{xy} = \frac{K_1^0}{\sqrt{2r}} \operatorname{Re} \left(\frac{s_1}{\sqrt{\cos \theta + s_1 \sin \theta}} \right). \tag{34b}$$

Therefore, it is proved that the asymptotical values for the interaction effect are really existent when setting $\beta_1 = 1$ and $\beta_2 \rightarrow \infty$. The tendency of the values are shown in Table 3.

It is also found from Figs 3 and 4 that the interaction effect may be either increased, i.e. the so-called amplification effect corresponding to $K_1^{MA}/K_1^0 > 1$, or decreased, i.e. the so-called shielding effect corresponding to $K_1^{MA}/K_1^0 < 1$. However, the transition from a shielding to an amplification effect is dependent not only on the position of the micro-crack (d/a_1), but also on the parameter of orthotropic material.

The numerical results for the so-called neutral-shielding angle α_N for which the transition occurs against the values of $\beta_1\beta_2$ are shown in Fig. 5 and Table 4, respectively, assuming d/a_1 to be a constant.

It is noted that the influence of the orthotropic parameter $\beta_1\beta_2$ on the angle α_N is very large in the range of $\beta_2 < 2$ and $\beta_1 = 1$ and that the influence decreases when β_2 increases. Moreover, it seems that an asymptotical value of the angle α_N exists when $\beta_1 = 1$ and $\beta_2 \rightarrow \infty$.

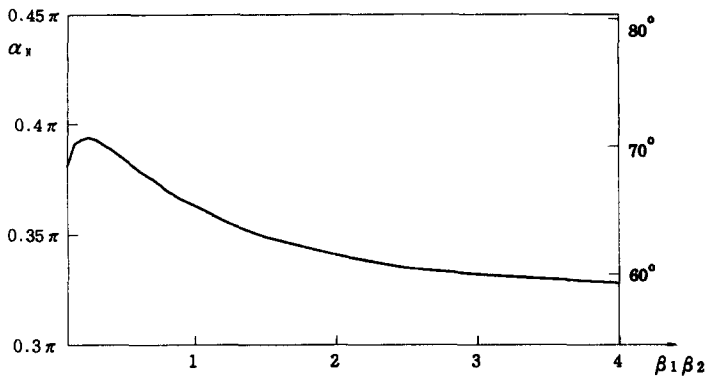


Fig. 5. The neutral angle α_N against the orthotropic parameters β_1 and β_2 assuming $s_1 = i\beta_1, s_2 = i\beta_2, a/a_1 = 100, d/a_1 = 2,$ and $\beta_1 = 1.$

Table 4. The neutral angle α_N against the orthotropic parameters assuming $S_1 = i\beta_1, S_2 = i\beta_2, a/a_1 = 100, d/a_1 = 2$ and $\beta_1 = 1$

$\beta_1\beta_2$	0.125	0.250	0.500	0.750	1.00001	1.250	1.500	2.000	2.500	3.000	3.500	4.000
α_N	0.3888π 69.98°	0.3937π 70.87°	0.3841π 69.14°	0.3726π 67.07°	0.3626π 65.26°	0.3548π 63.86°	0.3487π 62.77°	0.3405π 61.29°	0.3350π 60.30°	0.3315π 59.67°	0.3295π 59.31°	0.3275π 58.95°

To enhance the present investigation, a particular material system, i.e. 8-ply uni-directional graphite–epoxy laminate fabricated from Hercules AS-4-3501-06 tapy, is chosen which was used by Binienda *et al.* (1991). The material constants are

$$\begin{aligned}
 E_{11} &= 21.08e + 6\text{psi} \\
 E_{22} &= 1.5e + 6\text{psi} \\
 G_{12} &= 0.98e + 6\text{psi} \\
 \nu_{12} &= 0.3.
 \end{aligned}
 \tag{35}$$

The characteristic roots are purely imaginary when two preferred directions of the material coincide with the reference axes :

$$\begin{aligned}
 S_1 &= i\beta_1 \\
 S_2 &= i\beta_2
 \end{aligned}
 \tag{36}$$

where

$$\begin{aligned}
 \beta_1 &= 4.49611067 \\
 \beta_2 &= 0.83378232
 \end{aligned}
 \tag{37}$$

or

$$\begin{aligned}
 \beta_1 &= 1.19935381 \\
 \beta_2 &= 0.22241444
 \end{aligned}
 \tag{38}$$

for 90° transformation of the axes.

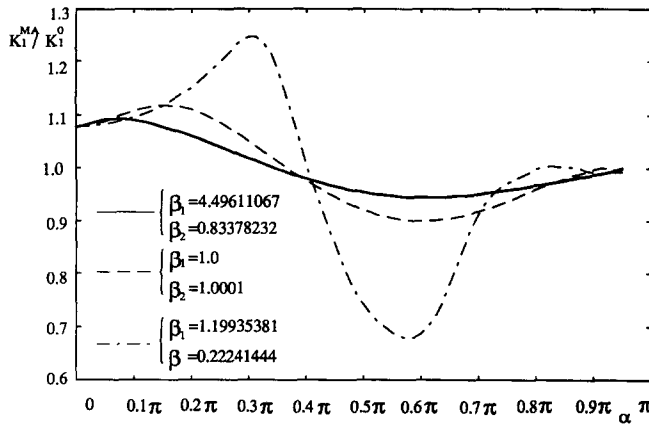


Fig. 6. Comparison of the interaction effect for a typical orthotropic material with those for an isotropic material.

Numerical results are shown in Fig. 6 for three kinds of roots (37), (38) and $\beta_1 = 1$, $\beta_2 \approx 1$ (isotropic case). It is found that the main-micro-crack interaction effect may be either amplification ($K_I^M/K_I^0 > 1$) or shielding ($K_I^M/K_I^0 < 1$) which seems to be dependent mainly on the local angle α and the characteristic roots. It is noted that the high strength fibre-reinforced composite is not always of advantage in this interaction problem for decreasing the amplification effect and increasing the shielding effect. For example, the amplification effect corresponding to the roots (38) is shown to be much larger than those corresponding to the roots (37) and the isotropic case in the range of α between 0.15π and 0.40π . However, the shielding effect corresponding to the roots (18) is also shown to be much larger than those corresponding to other two kinds of the roots in the range of α between 0.40π and 0.70π . Finally, it is noted also that the so-called neutral shielding angle α_N corresponding to the two orthotropic cases really diverges from those corresponding to the isotropic cases.

6. CONCLUSION AND REMARKS

(1) The orthotropic parameter $\beta_1\beta_2$ with $\beta_1 = 1$ has no influence on the main-micro-crack interaction effect K_I^M/K_I^0 when the main- and micro-cracks are collinear along the axis of material symmetry and the main-crack is under purely Mode I loading conditions.

(2) The influence of the parameter on the interaction effect is small when the micro-crack is little diverged from the collinear situation. However, significant influence on the effect could be induced when the micro-crack is far apart from the collinear situation, for example, $\alpha > 9^\circ$ for the cases of $\beta_1 = 1$ and $\beta_2 > 1$ or $\alpha > 18^\circ$ for the cases of $\beta_1 = 1$ and $\beta_2 < 1$.

(3) There are asymptotical values for the influence of the orthotropic parameter $\beta_1\beta_2$ on the interaction effect when setting $\beta_1 = 1$ and $\beta_2 \rightarrow \infty$.

(4) The neutral-shielding angle α_N is sensitively dependent on the orthotropic parameter $\beta_1\beta_2$ when $\beta_1 = 1$ and $\beta_2 < 2$. The dependence decreases when β_2 increases from 2.

(5) The high strength fibre-reinforced composite is not always of advantage in the interaction problem, whether the orthotropic nature of the composite decreasing the amplification effect or increasing the shielding effect is dependent not only on the characteristic roots, but also on location angle α .

REFERENCES

- Binienda, W., Wang, A. S. D. and Delale, F. (1991). Analysis of bent crack in unidirectional fibre reinforced composites. *Int. J. Fract.* **47**, 1–24.
 Bowie, O. L. and Freese, C. E. (1972). Central crack in plane orthotropic rectangular sheet. *Int. J. Fract. Mech.* **8**, 49–57.

- Chen, Y. Z. (1984a). General case of multiple crack problems in an infinite plate. *Engng Fract. Mech.* **20**, 591–597.
- Chen, Y. Z. (1984b). Multiple crack problems of antiplane elasticity in an infinite body. *Engng Fract. Mech.* **20**, 767–776.
- Chen, Y. H. and Hahn, G. H. (1989). Interaction of a stiffener with a crack in an anisotropic sheet. *Engng Fract. Mech.* **33**, 887–895.
- Chudnovsky, A. and Kachanov, M. (1983). Interaction of a crack with a field of microcracks. *Appl. Engng Sci.* **21**, 1009–1018.
- Chudnovsky, A. and Kachanov, M. (1983). *Appl. Engng Sci.* **21**, 1009–1018.
- Chudnovsky, A., Dolgopolsky, A. and Kachanov, M. (1987). Elastic interaction of a crack with a micro-crack array—part I and II. *Int. J. Solids Structures* **23**, 1–21.
- Chudnovsky, A. and Wu, S. (1991). Elastic interaction of a crack with a random array of micro-cracks. *Int. J. Fract.* **49**, 123–140.
- Erdogan, F. (1978). Mixed boundary value problems in mechanics. *Mechanics Today*, Vol. 4, pp. 1–86. Pergamon Press, Oxford.
- Gong, S. X. and Horii, H. (1989). General solution to the problem of micro-cracks near the tip of a main-crack. *J. Mech. Phys. Solids* **37**, 27–46.
- Gong, S. X. and Meguid, S. A. (1991). On the effect of the release of residual stresses due to near-tip microcracking. *Int. J. Fract.* **52**, 257–274.
- Gross, D. (1982). Spannungintensitätsfaktoren von ribsystemen (stress intensity factor of systems of cracks). *Ing. Arch.* **51**, 301–310.
- Hoagland, R. G. and Embury, J. D. (1980). A treatment of inelastic deformation around a crack tip due to microcracking. *J. Am. Ceram. Soc.* **63**, 404–416.
- Horii, H. and Nemat-Nasser, S. (1985). Elastic fields of interacting inhomogeneities. *Int. J. Solids Structures* **21**, 731–745.
- Horii, H. and Nemat-Nasser, S. (1987). Interacting micro-cracks near the tip in the process zone of a macro-crack. *J. Mech. Phys. Solids* **35**, 601–629.
- Hwu, C. (1991). Collinear cracks in anisotropic bodies. *Inter. J. Fract.* **52**, 239–256.
- Kachanov, M. (1993). Elastic solids with many cracks and related problems. *Adv. Appl. Mech.* **30**, 259–428.
- Lekhnitskii, S. G. (1963). *Theory of Elasticity of an Anisotropic Body*. Holden-Day, San Francisco.
- Rose, L. R. F. (1986). Micro-crack interaction with a main-crack. *Int. J. Fract.* **31**, 233–242.
- Sih, G. C. and Chen, E. P. (1981). Cracks in composite materials. *Mech. Fract.* **6**, 1–99.
- Sih, G. C. and Liebowitz, H. (1968). Mathematical theories of brittle fracture. In *Fracture* (Edited by H. Liebowitz), pp. 67–190. Academic Press, New York.
- Ukadgaonker, V. G. and Naik, A. F. (1991a). Interaction effect of two arbitrarily oriented cracks—part I. *Int. J. Fract.* **51**, 219–230.
- Ukadgaonker, V. G. and Naik, A. F. (1991b). Effect of interaction of two arbitrarily cracks—Applications—part II. *Int. J. Fract.* **51**, 285–304.